IEEE Access
Multidisciplinary | Rapid Review | Open Access Journal

Received April 23, 2019, accepted May 31, 2019, date of publication June 5, 2019, date of current version September 5, 2019.

Digital Object Identifier 10.1109/ACCESS.2019.2920862

An Approach to Extraction Midsagittal Plane of Skull From Brain CT Images for Oral and Maxillofacial Surgery

WENJUN TAN[1,2,5], YING KANG[4], ZHIWEI DONG[3], CHAO CHEN[7], XIAOXIA YIN[5], YING SU[4], YANCHUN ZHANG[5,6], LI ZHANG[3] AND LISHENG XU[4], (Senior Member, IEEE)

[1]Key Laboratory of Intelligent Computing in Medical Image, Ministry of Education, Northeastern University, Shenyang 110189, China
[2]School of Computer Science and Engineering, Northeastern University, Shenyang 110189, China
[3]Department of Oral and Maxillofacial Surgery, General Hospital of Shenyang Military Command, Shenyang 110819, China
[4]Sino-Dutch Biomedical and Information Engineering School, Northeastern University, Shenyang 110819, China
[5]Cyberspace Institute of Advanced Technology, Guangzhou University, Guangzhou 510000, China
[6]Centre for Applied Informatics, College of Engineering and Science, Victoria University, Melbourne, VIC 8001, Australia
[7]Academy of Medical Engineering and Translational Medicine, Tianjin University, Tianjin 300072, China

Corresponding author: Lisheng Xu (xuls@bmie.neu.edu.cn) and Li Zhang (jun1983@163.com)

ABSTRACT To prepare for the oral and maxillofacial surgery for the facial symmetry of patients, midsagittal plane of skull in brain computed tomography (CT) images is calculated with points manually chosen from skull by doctor. But the extracted midsagittal plane of the skull is different by different doctor. Even the extracted midsagittal plane of the same patient is also different by the same doctor in different times. The manually extracting operation usually takes a long time to increase the doctor's workload. Aimed at this problem, a semi-automatic extracting method for midsagittal plane of skull is proposed in this paper. First, the brain tissue is extracted by region growing method and the oriented bounding box (OBB) of the brain tissue is built. Second, the middle symmetry plane of the OBB of brain tissue is extracted as the initial midsagittal plane, which is updated by the mathematical translation and rotation method. Finally, the symmetrical characteristic of the brain tissue based on the updated symmetry plane is calculated by the mutual information method. This procedure is executed iteratively until the symmetrical characteristic of the brain tissue based on the new symmetry plane is no more different from the previous result. The final extracted symmetry plane is the midsagittal plane of skull in brain CT images of the patient. The midsagittal plane which is extracted manually by doctor is used to compare and evaluate the accuracy of this semi-automatic extracting symmetry plane method. The experimental results from both qualitative and quantitative analyses showed that the method can reach or approach the accuracy of manual extracted, but the stable level of this method is significantly higher than the manual method and this method can shorten the operate time to reduce the doctor's workload.

INDEX TERMS Oral and maxillofacial surgery, head symmetry plane, oriented bounding box (OBB), mutual information.

I. INTRODUCTION

In daily-clinical practice, traffic accidents may lead to damages on oral and maxillofacial tissues, which may result in the loss of function and badly deformation of oral and maxillofacial. For example, some facial collapses would be observed obviously when it collapses to a certain extent, some eating obstacles would arise due to the loss of oral and maxillofacial organs and some damages on skull may even be life-threatening [1]–[3]. The oral and maxillofacial surgery is an effective and important operation method for the tumors, wounds and malformations in oral and maxillofacial tissues [4]–[7]. When establishing an oral and maxillofacial surgery plan for patients with craniofacial asymmetry using 3D cephalometric analysis, construction of the midsagittal plane(MSP) of skull is the basis of the mandibular reconstruction, orthognathic surgery, maxillofacial trauma and temporomandibular joint reconstruction [8], [9].

In most current clinical applications, the extraction of MSP of skull is reconstructed manually in brain scans by oral and

The associate editor coordinating the review of this manuscript and approving it for publication was Jiachen Yang.

maxillofacial surgeons. This takes a lot time and requires expertise and suffers from interexpert variability, which can have a substantial effect on targeting in image guided oral and maxillofacial surgery. In previous studies, two manual extracting methods are developed and widely used to construct the MSP of skull in the 3D images [10]–[12]. The first involved the MSP of skull with three points on the midline of the head. These three points had to be some distance away from each other [13], [14]. The second method was to construct a plane that passed through a point on the midline of the head and was perpendicular to the horizontal plane [10], [15]. In these manual extracting methods, the points of skull are chosen manually from the CT images by doctor and the MSP of the skull is calculated by particular equations. If the surgeon observes that the symmetry plane of skull is not correct, the feature points would be repeatedly selected and the symmetry plane of the head is recalculated. These manually choosing and calculating steps are repeated over a few times until the new symmetry plane of skull is correct. And the extracted MSP of skull of a patient may be different by different doctors. Even it is also different at different times by a doctor. Furthermore, in patients with craniofacial asymmetry, the craniofacial structures are likely to lack symmetry. Thus, constructing the MSP of skull in patients with craniofacial asymmetry is very difficult, because the reference for determining the points with ideal symmetry or that passes correctly through the middle of the craniofacial area among the points used for determining the MSP of skull isn't correctly acquired before constructing it in these patients.

Therefore, a robust and accurate automatic extraction method of MSP of skull can be useful not only in research, but in clinical practice [16], [17]. However, detecting the symmetry plane of skull is difficult due to various noise artifacts, pathologies and tilted head scans [18]. A few algorithms for the detection of MSP of skull have been reported in the literatures in which most of the works are concentrated a geometric plane that separates the two hemispheres of the cerebrum by the interhemispheric fissure in order to detect the symmetry plane of skull, which is estimated as a same symmetry plane passing through those hemispheres [10]. Because the skull symmetry as a constraint has been included as an important anatomical feature for evaluating cerebrum asymmetry.

In general, the present methods used for MSP detection follow either a feature-based approach or a symmetry-based approach [19]. In the first type of approaches, the aim is to directly determine the inter-hemispheric plane from its intensity and textural features. Brummer [20] proposed an extraction approach by 3D extension of Hough transform to detect MSP that appears as long lines in the coronal view, and this approach involves detection of lines from the edge maps of 2D brain images and then detecting MSP by fitting a plane in brain volumes. Baji [21] proposed a method to locate MSP based on the computation of the different local texture between interhemispheric fissure region and the surrounding tissue. Ramasamy [22] presented a learning-based method for automatic and efficient localization of these landmarks and the plane using regression forests. Given a point in an image, this method first extracts a set of multi-scale long-range contextual features. Then the random forests models are built to learn a nonlinear relationship between these features and the probability of the point being a landmark or in the plane. Jayasuriya [23] proposed a method for identifying symmetry plane in 3D brain MRI images, based on the analysis using fractal dimension and lacunarity. Ekin [24] tried to extract midsagittal plane for by the feature points that correspond to the interhemispheric fissure and outlier-robust RANSAC algorithm, which is applied for fitting a mid-sagittal line. A line fitting algorithm is developed to detect the MSP by Hu [25]. Volkau [26] extracted the MSP using the calculation of the Kullback and Leibler measures to characterize the difference between two distributions. A method to segment brain volumes into left and right cerebral hemispheres using the Graph Cuts algorithm is developed by Liang [27]. Song [28] determined the MSP based on a group of assistant parallel lines and correlation of gravitational forces. Bergo [29] developed a heuristic maximization method to detect the MSP, which assumed that the MSP contains the maximum area of Cerebrospinal Fluid when ventricles are excluded. Teverovskiy [30] proposed an intensity method based on cross correlation technique. This method performs the cross correlation on an edge image in order to capture the anatomical structures of the brain and skull while ignoring intensity fluctuation and found the MSP accurately on brain images. An automation method to find the MSP based on the KL measure from MR brain images was devised in Kuijf [31]. Wu [32], [33] presented a fast and robust MSP extraction method based on 3D scale invariant feature transform (SIFT), which mainly rely on the gray similarity, 3D edge registration or parameterized surface matching to determine the fissure plane based on distinctive 3D SIFT features. A learning-based method for automatic and efficient localization of the MSP using regression forests is developed by Liu [34]. Given a point in an image, this method first extracted a set of multiscale long-range contextual features. Then the random forests models are built to learn a nonlinear relationship between these features and the probability of the point being a landmark or in the plane. Automatic segmentation of MSP using curve fitting was developed by Kalavathi [35]. Schwing [36] proposed an approach for mid-sagittal plane extraction based on hierarchical landmark detection. Jayasuriya [37] presented a novel technique for extracting the mid plane from volumetric magnetic utilizes anatomical and radiological properties.

In the second type of approaches, the MSP is defined as the plane that maximizes the similarity between the brain and its reflection. Ruppert [38] presented an approach for MSP extraction based on bilateral symmetry maximization. Ardekani [39] proposed an algorithm for the automatic detection of the mid-sagittal plane in 3D brain images. The algorithm seeks the plane with respect to which the image exhibits maximum symmetry. For a given plane, symmetry is

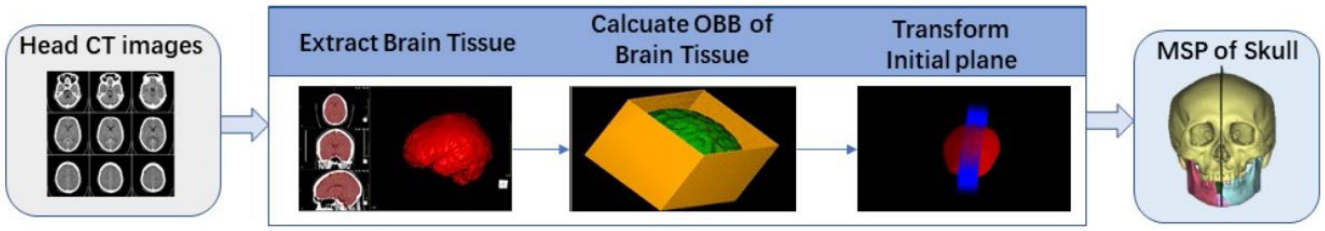

FIGURE 1. Overview of the proposed method's framework.

measured by the cross-correlation between the image sections lying on either side. The search for the plane of maximum symmetry is performed by using a multiresolution approach which substantially decreases computational time. Liu [40] developed an algorithm for extracting the axis of bilateral symmetry from each axial brain slice and combining results from multiple slices to determine the central plane of bilateral symmetry for the 3D head. Kruggel [41] proposed an MSP detection method by considering the symmetry plane as a first order approximation. An edge-based cross-correlation method was proposed by Liu [42] that separated the plane into 2D symmetry axis on each slice. Zhang [43] proposed a construction method for the MSP based on the principal component analysis for grey scale similarity. Rupper [38] extracted the optimal MSP with 3D Sobel edge operator and multiscale correlation. Tuzikov [44], [45] measured the similarity between the image and its reflection to obtain the MSP. Qi [46] developed an automated ideal midline estimation system using slice selection algorithm, edge detection and Hough transform. Prima [47] developed an iterative approach to find MSP. This method worked by assuming an initial guess of the MSP and updating it by computing the local similarity measures between the two sides of the head by applying the block matching procedure in brain images. Zhang [48] propose a method to automatically extract the Mid-sagittal Plane and re-alignment of 3D head image within the scanner coordinate system by tilt correction. This method expresses the problem of Mid-sagittal Plane extraction as a registration problem and compute a degree of similarity between the image and its reflection with respect to a plane. Stegmann [49] use a sparse set of profiles in the plane normal direction and maximize the local symmetry around these using a general-purpose optimizer to detect the MSP. Davarpanah [50] introduced a MSS extraction method, which used fractal dimension and lacunarity as two independent factors of the voxels' values in order to determine the symmetry degrees in each axial slice.

Although a variety of works have been made in both methodology and performance in addressing the issue of MSP detection, existing methods are still not reliable and accurate enough or fast to be used in brain scanning. Most of them relied on manual operation, which may easily suffer from image noise, skull shape or the deformation of edge. In addition, them are too time consuming to achieve real-time performance in clinical setting. Meanwhile, the automatic techniques of extraction of MSP are significant improvement for better applicability and accuracy. These automatic methods can eliminate the subjective error of doctors and reduce the operating time. However, due to eyeball, soft tissues and neck tissues besides the skull in brain images [51], it is difficult to automatically extracted MSP of skull in brain CT images.

Therefore, in this paper, we proposed an semi-automatic, fast, accurate, and robust extraction method of MSP of Skull in brain CT images. It does not rely on any preprocessing of the images such as edge enhancement or image denoising. We extract brain tissue for feature points in a patient's 3D brain CT images with region growing algorithm and obtain Oriented Bounding Box(OBB) of the brain tissue to build initial symmetric plane. Then we extract the MSP of the skull using mathematical transformation and the mutual information of this initial symmetric plane. We evaluate this method using a large clinical dataset of 10 patients. We also compare our method to the doctor's manual extraction method, which is a publicly available implementation of extraction approach for the MSP of the skull in clinical practice.

The rest of the paper is organized as follows. Section II describes the framework of our novel approach, including its design consideration and flowchart, and elaborates the theoretical basis and processing steps of this work. Experimental results and discussion are presented in Section III. Finally, Section IV concludes the paper.

II. METHODOLOGY

In this section, we propose the framework of this work. The framework consists of three components, as illustrated in Figure 1: the extraction algorithm of brain tissue in brain CT images, the build technology of initial symmetry plane based on OBB and the updated method of MSP of the skull. In the section on the brain tissue extraction, an algorithm for extracting the brain tissue based on region growing method is used in brain CT images. Generally, the brain CT images are divided into two categories of skull and brain tissue. The grayscale value of image pixel of brain tissue is lower than that of skull. A method based on OBB is developed to build the initial symmetry plane in the extracted brain tissue. Furthermore, we update the symmetry plane progressively with mutual information of the brain tissue. As a result, this approach guarantees that the MSP of the skull is

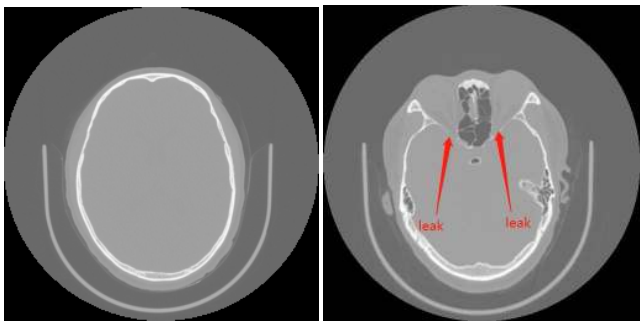

FIGURE 2. Different part of brain of CT images: (a) the upper part of brain tissue, (b) the lower part of brain tissue.

automatically and correctly extracted on the OBB of the brain tissue and achieves a more vivid effect.

A. BRAIN TISSUE SEGMENTATION METHOD

According to the grayscale value of the brain CT images, the area of that are divided into two categories of skull and brain tissue, which grayscale value are significantly different in CT image. Region growing method can segment effectively and correctly a specific set of gray values in an image based on the gray-scale difference between pixel of that image. The region growing method is an iterative image segmentation method with three elementary parts: seed points selection, definition of similarity, and criteria for convergence to terminate the iterative process [52]. The initial region begins as the exact location of the seeds. Then, the regions are grown from these seeds to adjacent points depending on a region membership criterion (e.g. grayscale intensity). Keep examining whether the adjacent points of seeds should be classified into the seed points until the criterion is not met any more [53].

In the brain CT images, the gray value of brain tissue is significantly higher than that of the skull and image surrounding background. But the eye area and brain tissue are high similarity in terms of the gray value. For this reason, segmentation of brain tissue using region growth method will also segment the eye area. Fortunately, in the upper part of brain of the CT image, there is no area such as eyes. Figure 2 shows brain CT images of the different parts: Figure 2(a) and Figure 2(b) are the upper part and the lower part of brain, respectively. According to the brain anatomy, the MSP of upper and lower part of brain are approximately same in the images. Therefore, we segment the upper part of brain in the images to extract its MSP as the MSP of whole brain tissue.

In this paper, a semi-automatic region growing method [53], [54] is used to segment the brain tissue in CT images. This method requires doctor to select a seed point manually in a particular image, which divides the brain into the upper part and lower part. It is easy to select this particular image and the centroid of isolated brain tissue regions of that as a seed point. The similarity definition is used to determine whether the unlabeled pixels are added to the detection region. This definition refers to the difference of image

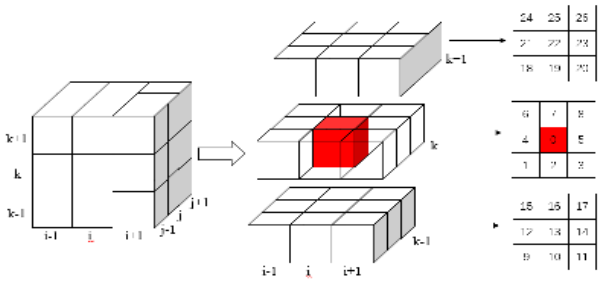

FIGURE 3. 26 neighborhoods of region growing.

intensity between the neighboring pixels. The similarity condition is formulated as follows:

$$|I(x_k, y_k) - I(x, y)| < \theta, \quad (x_k, y_k) \in N_{26} \tag{1}$$

The unlabeled voxel (x_k, y_k) in the 26-adjacent N_{26} can be added to brain tissue region, if the difference between the grayscale value of $I(x_k, y_k)$ and seed voxel $I(x, y)$ is less than the given threshold θ. And this voxel (x_k, y_k) is added to the seed queue voxel for next iteration. This process is shown in Figure 3.

Since this method relies on the difference between the grayscale value of the voxels in the 26 neighborhoods, the given threshold θ plays a decisive role in this process. The extraction brain tissue regions are different with different given threshold. Figure 4 shows the segmentated brain tissue regions for different thresholds. In this case, the best segmentation result is when the given threshold is 50. Finally, the pixels of segmented brain tissue and other tissues are marked 1 and 0 in the CT images, respectively.

B. EXTRACT INITIAL SYMMETRY PLANE OF BRAIN TISSUE BASED ON ORIENTED BOUNDING BOX METHOD

The basic idea of the oriented bounding box(OBB) algorithm is to replace the complex geometric objects with a slightly larger and simpler geometry as a bounding box. It is one of the important methods for the preliminary detection of collision interference [55]. According to its characteristics, it is used to extract the initial symmetry plane in this paper. The extracting steps of the OBB bounding box of the upper part of brain tissue are as follows.

If the whole pixels of segmented brain tissue are be used to calculate the OBB bounding box, the computation time is very long. So the coordinates of the boundary pixels of the segmented brain tissue are searched by row scan method in this work.

Assuming that each object consists of a triangle, the first-order (mean) and second-order (covariance matrix) statistical properties of the vertex coordinates of the object are used to calculate the position and orientation of the OBB. The set of triangle vertices is regarded as a three-variable probability distribution function. When calculating the OBB bounding box, the mean and the covariance matrix of the triangle vertices are used to calculate the center position and direction of the bounding box. Let the vertex vector of the i-th triangle of the set of triangles be p[i], q[i]

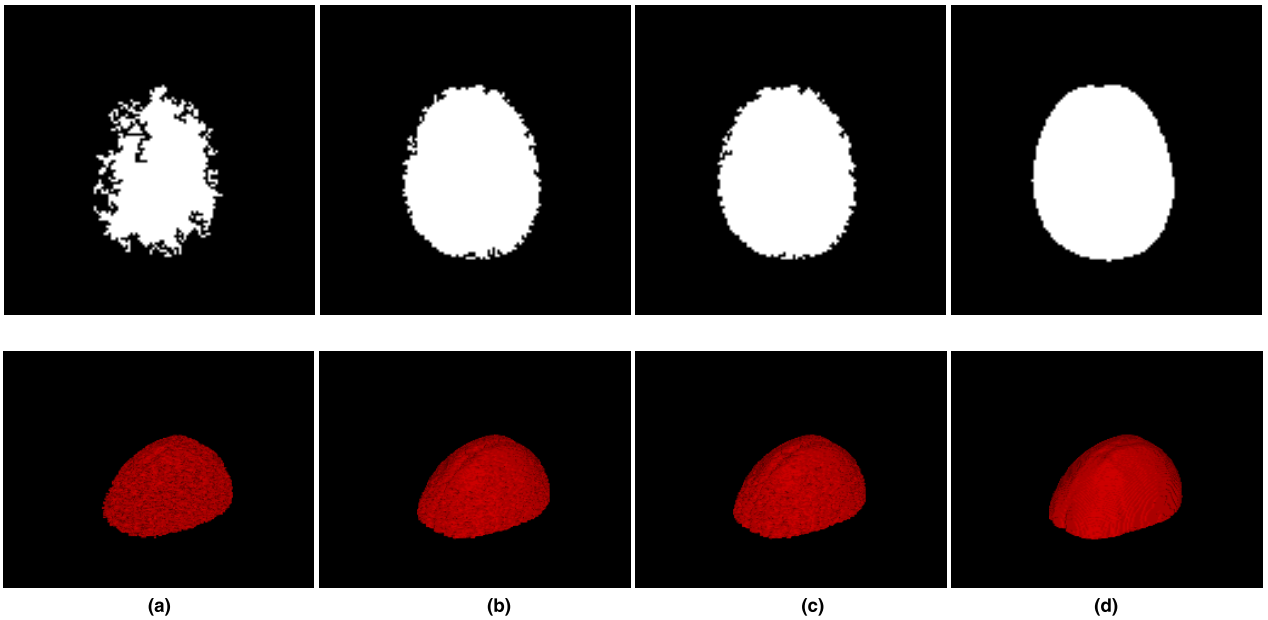

FIGURE 4. The segmentation result of brain tissue with different given thresholds: (a) sementation result with 10 threshold, (b) sementation result with 20 threshold, (c) sementation result with 40 threshold, (d) sementation result with 50 threshold.

and r[i], the number of triangles of the bounding box be n, and the subscripts j and k represent the components of (x, y, z).

The mean of the vertices of the triangle patch is as follow:

$$u = \frac{1}{3n}\sum_{i=1}^{n}\left(p^i + q^i + r^i\right) \tag{2}$$

The elements of the covariance matrix are as follow:

$$D_{jk} = \frac{1}{3n}\sum_{i=1}^{n}\left(\overline{p_j^i p_k^i} + \overline{q_j^i q_k^i} + \overline{r_j^i r_k^i}\right), \quad 1 \le j, k, \le 3 \tag{3}$$

$$\begin{cases} \overline{p^i} = p^i - u \\ \overline{q^i} = q^i - u \\ \overline{r^i} = r^i - u \end{cases} \tag{4}$$

The three eigenvectors of the covariance matrix are obtained from the numerical calculation, and the eigenvectors are unitized as a base. Since it is a symmetric matrix, the eigenvector bases are orthogonal to each other. Assuming the matrix is C, the direction axes of the OBB bounding box can be determined using the three feature vectors of C.

If the OBB is calculated by using the triangle vertices, the amount of this calculation is a large burden so that it takes a long time. For reducing the amount of computation, this paper proposes an improved OBB algorithm based on by using the above segmentation of brain tissue regions based on the original OBB algorithm. The main idea of the improvement of the OBB algorithm is that the boundary points of the brain tissue region are used to replace the triangular patch points in this paper.

The main steps of the improved OBB algorithm in this work are as follows:

1) Obtain the boundary points of brain tissue

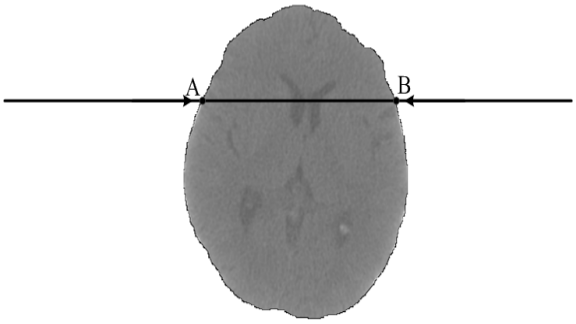

FIGURE 5. Obtain the boundary points of the brain tissue by the layer-by-layer progressive search.

The pixels of segmented brain tissue and other tissues are marked 1 and 0 in the CT images, respectively. According to the marked value of the segmented brain tissue, we search from both sides (as shown in Figure 5) until the first 1 occured. Search rules are as follows:

$$\begin{aligned} &if \ \ (P_i) = 1, \\ &\quad P_i \ is \ boundary \ point; \\ &else \\ &\quad contiune \ to \ search; \end{aligned} \tag{5}$$

In which, p_i is the point of the CT image. The algorithm uses the layer-by-layer progressive search to obtain the boundary points of the brain tissue, as shown in Figure 5.

The two points A and B represent the two boundary points of the line, point A is the boundary point searched from left to right, and point B is the search result in the reverse direction. All rows of CT brain image data have two vertices per line,

and the vertex coordinate set is equivalent to the triangular patch set in the OBB algorithm.

2) Calculate the mean coordinate and the covariance matrix of the vertex coordinate set

The mean coordinates of the vertex coordinate set is calculated by Equation (6).

$$(\mu_x, \mu_y, \mu_z) = \frac{1}{n}\left(\sum_{i=1}^{n} p_i(x), \sum_{i=1}^{n} p_i(y), \sum_{i=1}^{n} p_i(z)\right) \quad (6)$$

In which, (μ_x, μ_y, μ_z) is the mean coordinates of the vertex coordinate set and $(p_i(x), p_i(y), p_i(z))$ is the coordinates of the i-th boundary point.

The covariance matrix of the vertex coordinate set is calculated as Equation (7).

$$\begin{cases} C_{jk} = \dfrac{1}{n}\displaystyle\sum_{i=1}^{n} \overline{p_j^i p_k^i} \\ \overline{p_j^i} = p_j^i - \mu_j \\ \overline{p_k^i} = p_k^i - \mu_k. \end{cases} \quad (7)$$

In which, C_{jk} is the covariance of the vertex coordinate points, j and k correspond to the x, y and z coordinate, respectively. The corresponding covariance matrix is as follows:

$$\begin{bmatrix} c_{xx} & c_{xy} & c_{xz} \\ c_{yx} & c_{yy} & c_{yz} \\ c_{zx} & c_{zy} & c_{zz} \end{bmatrix} \quad (8)$$

3) Calculate three eigenvectors of the covariance matrix

The eigenvectors of the covariance matrix are converted to standard orthogonal basis, which are the direction of the three coordinate axes of the bounding box. The new coordinate direction generally does not coincide with the Cartesian coordinate system.

The X, Y axis represents the direction axis in the Cartesian coordinate system, and the X', Y' axis represents the new direction axis of the brain tissue, as shown in Figure 6.

The extreme points on the new coordinate axis are calculated based on the projection point values of the respective boundary points in the coordinate direction. In this work, $X'\max - X'\min$, $Y'\max - Y'\min$ and $Z'\max - Z'\min$ represent the extreme points of the sagittal, coronal and cross direction of the new direction axis of the brain tissue, respectively. The length, width and height of the OBB are calculated according to the as Equation (9).

$$\begin{aligned} OBB.width &= X'\max - X'\min \\ OBB.length &= Y'\max - Y'\min \\ OBB.height &= Z'\max - Z'\min \end{aligned} \quad (9)$$

Figure 7 shows that the extracted OBB of the upper part of brain tissue by the above method. And the symmetry plane in the x direction as the initial symmetry plane of the upper part of brain tissue, which is shown in Figure 8. The initial symmetry plane divides the upper part of brain tissue into two parts, which are approximately symmetrical parts.

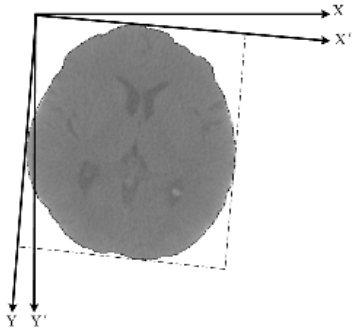

FIGURE 6. Axis of OBB of brain tissue.

C. EXTRACT THE ACCURATE SYMMETRY PLANE OF BRAIN TISSUE BASED ON ORIENTED BOUNDING BOX METHOD

Although the initial symmetry plane of the upper part of brain tissue is extracted by OBB method, the symmetry plane is not accurate. In this work, the mathematical translation and mutual information method is used to get the accurate symmetry plane. The initial symmetry plane is performed translation and rotation transformation continuously within ten pixels of the initial plane. The mutual information of the new left and right parts of the brain tissue is calculated with each transformation step. Then, the symmetry plane with maximum value of mutual information is the optimal symmetry plane of the upper part of brain tissue. Finally, according to the same symmetry plane of the brain tissue and skull, this optimal symmetry plane of the upper part of brain tissue is as the symmetry plane of the skull.

1) MUTUAL INFORMATION METHOD

Mutual information is usually used to describe the statistical correlation between two systems, or to describe how much information is the same with another [56], [57]. The value of mutual information is closely related to entropy, which is used to represent the complexity and uncertainty of a system. For a grayscale image, its grayscale value is regarded as a random variable. The grayscale value of each point is used as an event in one random variable, and the occurrence of grayscale value of each level is calculated according to the grayscale information of an image The probability of an image can be defined as Equation (10), where h_i is the number of pixels with gray value i and N is the total number of pixels.

$$p_i = \frac{h_i}{N} \quad (10)$$

The joint entropy $H(A, B)$ is a statistical measure of the correlation between the random variables A and B [59]. For two random variables A and B, their probability distribution are $p_A(a)$ and $p_B(b)$. And their joint probability distribution is described as $p_{AB}(a, b)$, $H(A, B)$ can be calculated as Equation(11-13). Mutual information is calculated with the value of entropy and joint entropy as Equation(14).

$$H(A) = -\sum_{a} p_A(a) \log p_A(a) \quad (11)$$

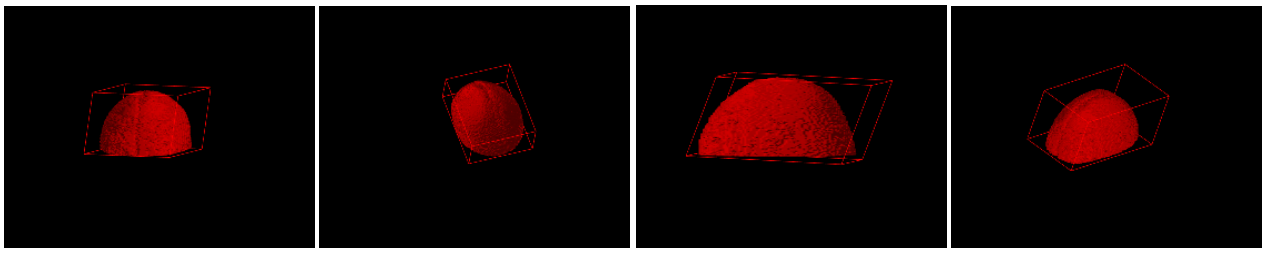

FIGURE 7. OBB of the upper part of brain tissue.

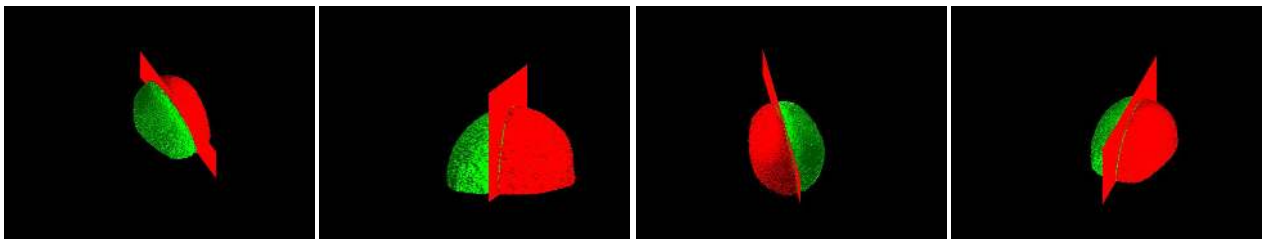

FIGURE 8. The initial plane of symmetry of the upper part of brain tissue based on the OBB method.

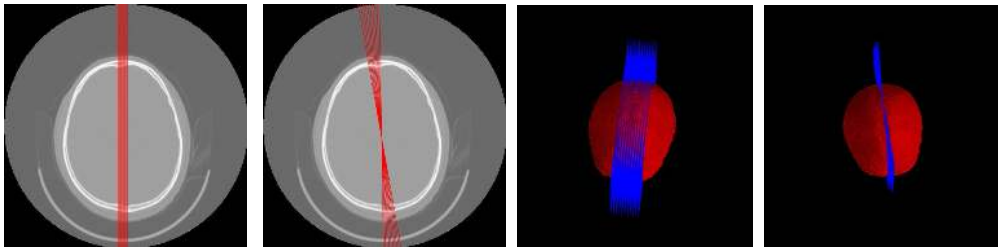

FIGURE 9. Translation and rotation within 10 pixels: (a) translation in 2D view; (b) rotation in 2D view; (c) translation in 3D view, (d) rotation in 3D view.

$$H(\mathrm{B}) = -\sum_{b} p_B(\mathrm{b}) \log p_B(\mathrm{b}) \tag{12}$$

$$H(A, B) = -\sum_{a,b} p_{AB}(a, b) \log p_{AB}(a, b) \tag{13}$$

$$I(A, B) = H(A) + H(B) - H(A, B) \tag{14}$$

2) MATHEMATICAL TRANSLATION AND ROTATION

The initial symmetry plane of the upper part of brain tissue basically determines the range of the final symmetry plane. To obtain the accurate symmetry plane of the skull, the mathematical translation and mutual information method is used based on the initial symmetry plane.

CT Image coordinate system and world coordinate system are different. Firstly, this work transforms the two coordinate system. The resolution, the origin of coordinates and the layer thickness are all stored in CT image files. Using these information, the two coordinate systems are transformed as Equation(15-17), where $pixelX$, $pixelY$ and $pixelZ$ are the image coordinate of the target point, and $worldX$, $worldY$ and $worldZ$ are the corresponding world coordinates of the target point. $PixelSpacing\_X$ and $PixelSpacing\_Y$ are the spatial resolution of pixel, $SliceLocation$ and is the slice location information of the point, $SliceThickness$ and is the thickness of a slice.

$$pixelX = worldX / PixelSpacing\_X \tag{15}$$

$$pixelY = worldY / PixelSpacing\_Y \tag{16}$$

$$pixelZ = \frac{worldZ - SliceLocation}{SliceThickness} + 1 \tag{17}$$

The projection of the initial symmetry plane on a CT image is a straight line, which is described as Equation(18). The translation and rotation transformation of the symmetry plane is expressed as Equation(19), where ξ and ζ are both small neighborhoods with a range of $[-5, 5]$. Positive value of ξ indicates the translation to the left while negative to the right. Positive value of ζ indicates the rotation in the counterclockwise direction while negative in the clockwise.

$$Y = kx + b \tag{18}$$

$$Y = \tan(90 + \zeta) \bullet (x + \xi) + b \tag{19}$$

In the above given range, translation and rotation operations are continuously performed. This process is shown

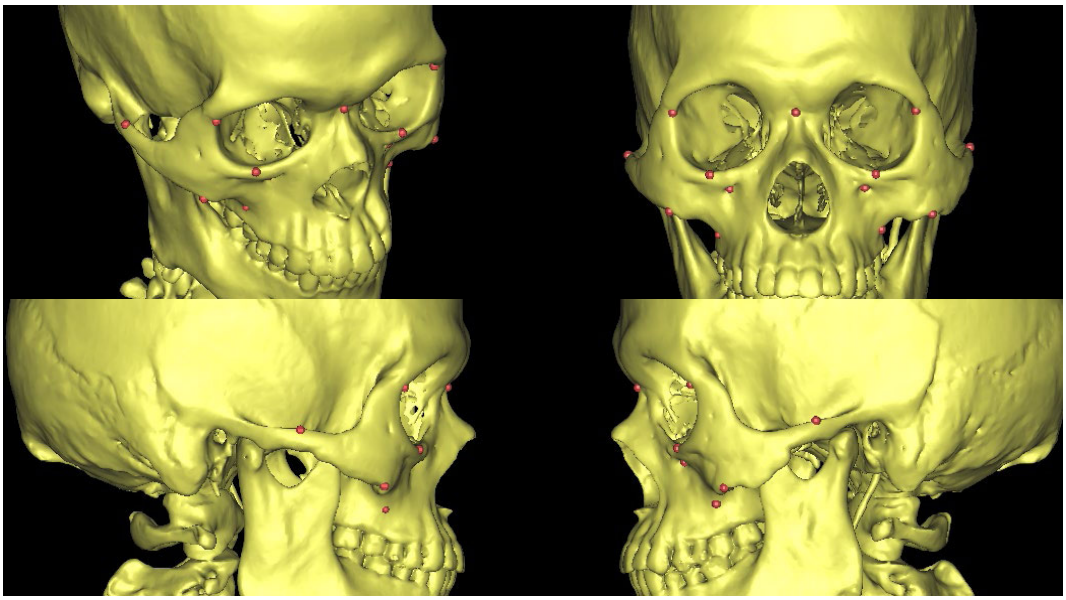

FIGURE 10. The 6 pairs of symmetry points of skull.

in Figure 9. Meantime, the mutual information value of the left and right brain tissue, which is divided by the new symmetry plane, is calculated. Finally, the symmetry plane with maximum mutual information is considered as the most accuracy symmetry plane of the brain tissue. According to the same symmetry plane of the brain tissue and skull, this symmetry plane is as the symmetry plane of the skull.

III. EXPERIMENTAL RESULTS AND DISCUSSIONS

In this section, we give a brief description of datasets, experimental settings, recognition accuracy, performance comparison and discuss the experimental results.

A. EXPERIMENTAL IMAGE DATASET AND SYSTEM

The 10 patients' head CT image dataset were used in this experiment with resolution of 512 × 512, slice thickness less than 1.5mm, which are from a same hospital. All of the 10 patients are male and their ages cover from 20 to 75. In order to protect patient privacy information, the image dataset hides the hospital's and patient's name. Refer to the previous research [8], [9], facial asymmetry index(FAI) is used to evaluate the accuracy of this method. The 6 pairs of symmetry points of skull are required to calculate FAI, as shown in Figure 10, which marks the points as red color. These symmetry points of each image dataset are manually marked by the doctor for each database as ground truth. FAI is calculated by these symmetry points as shown in Equation (20).

$$FAI = \sum_{i=1}^{12} |Rd_i - Ld_i| \tag{20}$$

where Ld_i and Rd_i is the distance from the left or right point of a pair of symmetry points to the extracted symmetry plane of skull by this method, respectively. The smaller the FAI is, the more accurate the symmetry plane of skull is.

Our system was implemented in Matlab 2015 on a PC with 4 Intel(R) Core is-i7-6700U CPUs 2.60 GHz, 8 GB DDR4 RAM and NVIDIA GeForce 940Mx GPU with 2 GB video memory.

B. EXPRIMENTAL RESULTS AND ANSLYSIS

This section discusses the accuracy of the proposed method from the following two aspects. On the one hand, the extracted symmetry plane of skull by this method is compared with the symmetry plane by doctor's manual extraction method. The comparison results of the 10 patients' head CT image dataset are shown in Figure11. The red and blue plane are the symmetry plane of skull extracted by the doctor and by this method, respectively. The experiment results show that the difference of the symmetry plane of skull extracted by the doctor and by this method is very small.

On the other hand, for quantitative comparison of the accuracy of the method, the FAI results of the doctor's manual extraction symmetry plane, the initial symmetry plane with OBB of brain tissue, the optimal symmetry plane using translation operation, the optimal symmetry plane using translation operation and the optimal symmetry plane of this method are calculated by the given 6 pairs of symmetry points of skull according to Equation(20). The results of FAI are shown in Table 1. And Figure 11 and Figure 12 show the FAI results by different methods.

The FAI of dataset 1, 4, 7, 8, 9, 10 by this method are smaller than the results by doctor manually marking. And the FAI of other datasets by this method are bigger than the results by doctor manually marking. The average FAI of the results

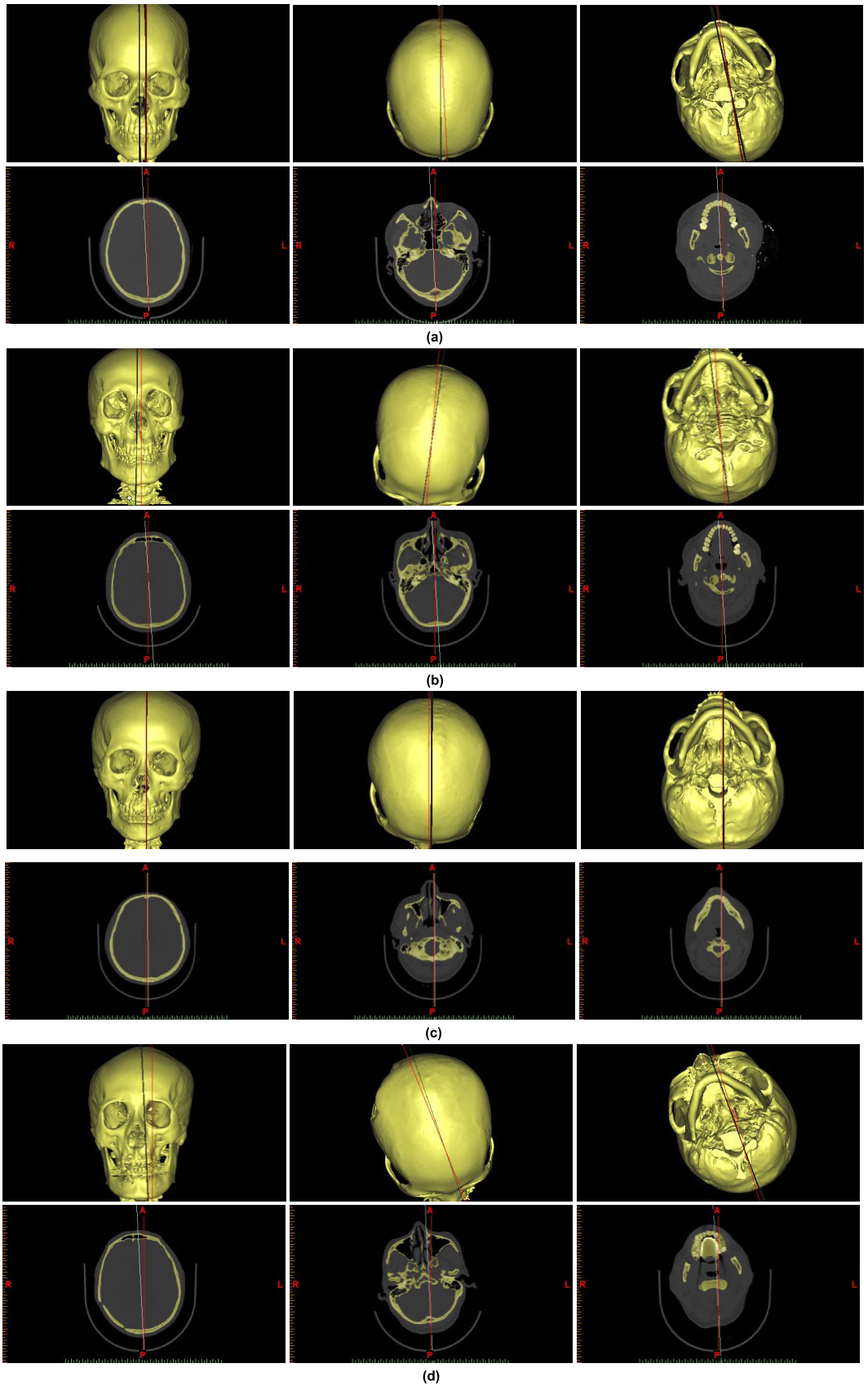

FIGURE 11. The comparison results of the 10 patients' head CT image datasets of doctor's manual method and this method: (a-i) figures are the result of the 10 patients' head CT image datasets.

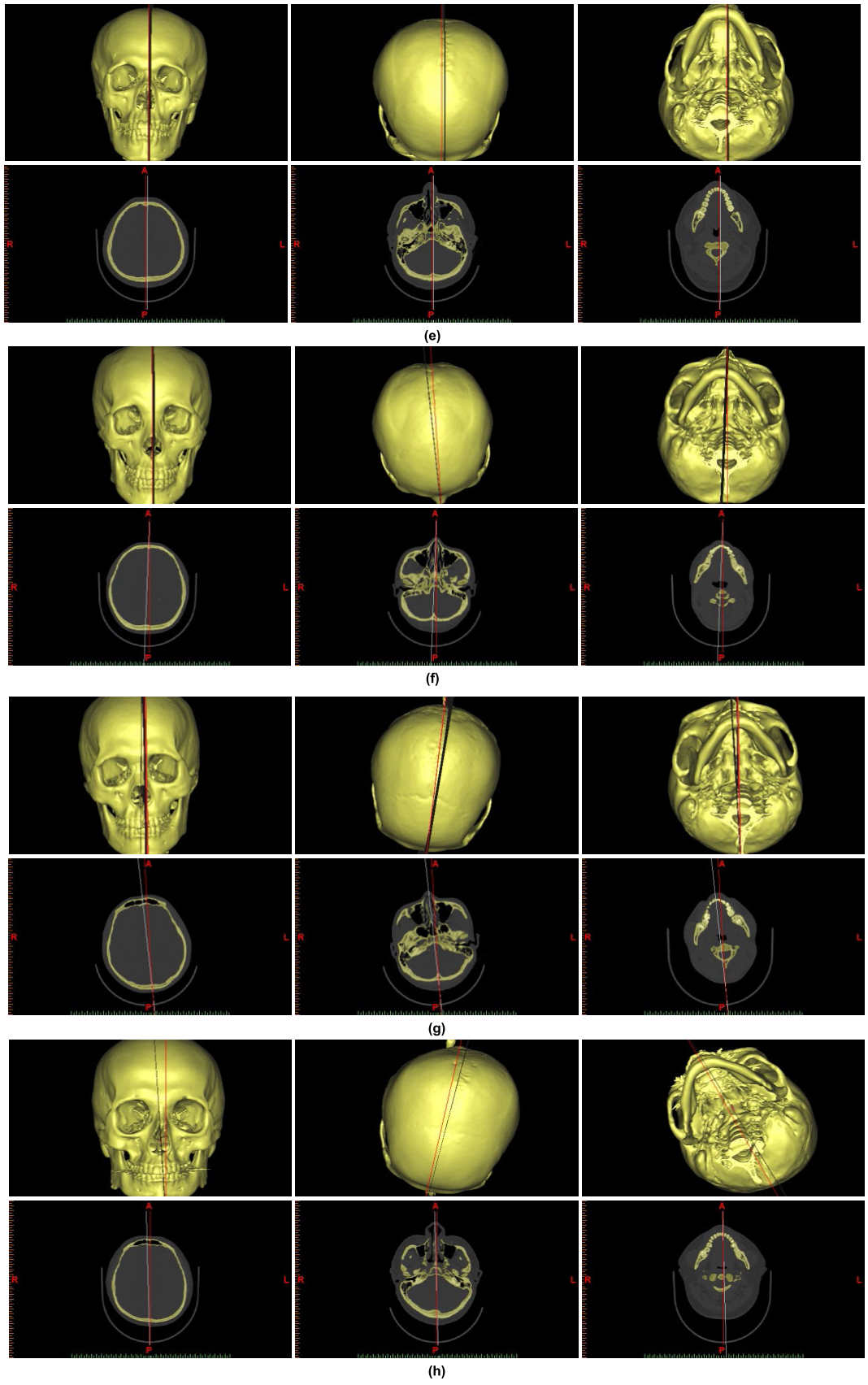

FIGURE 11. *(Continued.)* **The comparison results of the 10 patients' head CT image datasets of doctor's manual method and this method: (a-i) figures are the result of the 10 patients' head CT image datasets.**

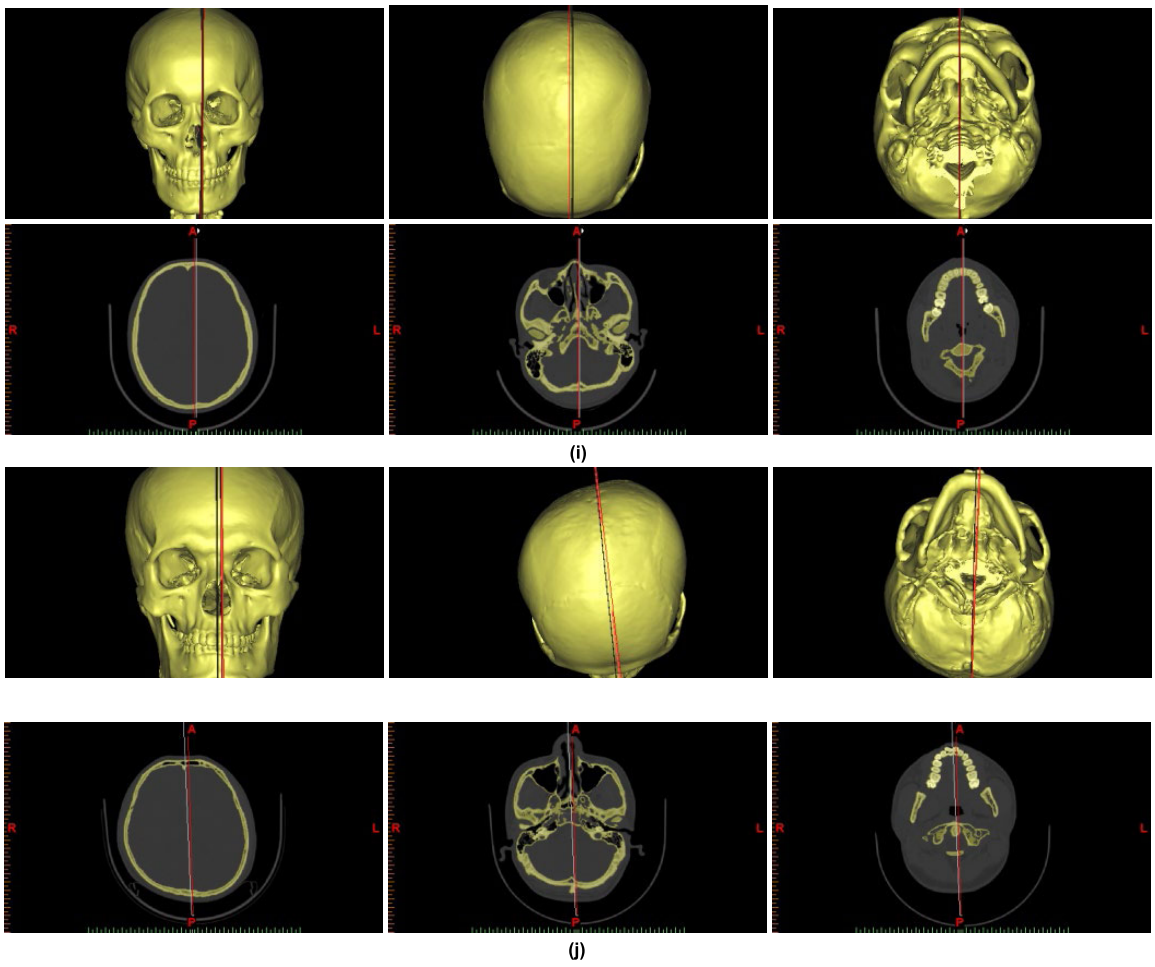

FIGURE 11. *(Continued.)* **The comparison results of the 10 patients' head CT image datasets of doctor's manual method and this method: (a-i) figures are the result of the 10 patients' head CT image datasets.**

TABLE 1. **The fai of extraction symmetry planes of different method.**

Dataset No.	Doctor's result	Initial plane	Translation operation	Rotation operation	This method
1	13.89	64.91	4.91	7.80	10.27
2	3.96	60.46	120.46	61.68	18.09
3	6.01	6.01	6.01	1.78	6.55
4	98.50	96.97	148.46	199.59	17.22
5	26.38	10.11	49.89	87.13	106.36
6	12.11	37.29	95.31	45.28	21.96
7	92.61	94.05	44.05	94.05	80.95
8	78.38	13.32	36.68	79.20	71.72
9	63.16	125.00	73.53	58.04	11.33
10	4.01	88.96	28.96	110.15	4.21
average	39.90	59.71	60.83	74.47	34.87

by doctor manually marking and the results by this method are about 39.90 and 34.87, respectively. This shows that the accuracy of this method is almost equal to the accuracy of the doctor's manual method.

To further verify the accuracy of the proposed algorithm, Student's T test [59] is used to compare the difference between the plane extracted by doctors and by this method. First, a hypothesis is established that there is not significantly

FIGURE 12. The FAI results by difference methods.

difference between the extraction results of the two methods. Student's T test is performed with the extracted results of the 10 patients' head CT image dataset by the two methods. In this test, the significance indicates whether this hypothesis is true. The calculation results show that $P = 0.273$, which proves that the hypothesis is true. It further shows that there is no significant difference between the accuracy of this method and the doctor's manual method.

In present, the extracted midsagittal plane of the skull is different by different doctor. Even the extracted midsagittal plane of the same patient is also different by the same doctor in different time. And the manual method usually takes a long time for doctors. However, the experiment results show that this method is an automatically extracting process that excludes the subjective factors of the doctor, and the robustness of this method is significantly better than the manual method.

Meanwhile, the average calculation time of this method is less than one minute, while the average calculation time of the manual method by doctor is about five minutes. This method can shorten the operate time to reduce the doctor's workload.

IV. CONCLUSIONS

The midsagittal plane of skull in brain CT images is required for the he oral and maxillofacial surgery for the facial symmetry of patients. In present, the midsagittal plane of skull is extracted by doctor manual operation, which usually takes a long time for doctors. Meanwhile, the extracted midsagittal plane of the skull is different by different doctor. Even the extracted midsagittal plane of the same patient is also different by the same doctor in different time. In this paper, a semi-automatic extracting method for midsagittal plane of skull is proposed based on region growing method, OBB bounding box and mutual information algorithm. The extracted symmetry plane of skull by this method is compared with the symmetry plane by doctor's manual extraction method. For quantitative analysis of the accuracy of the method, the FAI is used to evaluate the experiment results.

The FAI results show that some experiment results of this method are smaller than the results by doctor manually method. And the FAI of other datasets by this method are bigger than the results by doctor manual method. The average FAI of the results by doctor manual method and the results by this method are almost same. This shows that the accuracy of this method is almost equal to the accuracy of the doctor's manual method. But the stable level of this method significantly higher than the manual method and this method can shorten the operate time to reduce the doctor's workload.

ACKNOWLEDGEMENTS

The authors would like to thank the editor and reviewers for their valuable advices that have helped to improve the paper quality. Wenjun Tan and Ying Kang contribute equally to this work and should be regarded as joint first authors. Li zhang and Lisheng Xu contributed equally to this work, and should be regarded as joint corresponding authors. This

work is supported by the Fundamental Research Funds for the Central Universities(N181602014), National Key Research and Development Program of China(2018YFC1314501), National Natural Science Foundation of China (61806146).

REFERENCES

[1] K. Thankappan, N. P. Trivedi, P. Subash, S. K. Pullara, S. Peter, M. A. Kuriakose, and S. Iyer, "Three-dimensional computed tomography-based contouring of a free fibula bone graft for mandibular reconstruction," *J. Oral Maxillofacial Surg.*, vol. 66, pp. 2185–2192. Oct. 2008.

[2] R. Villar-Puchades and B. Ramos-Medina, "Virtual surgical planning for extensive fibrous dysplasia in the mandible," *Aesthetic Plastic Surg.*, vol. 38, pp. 941–945, Oct. 2014.

[3] J. T. van Gemert, R. J. van Es, A. J. Rosenberg, A. van der Bilt, R. Koole, and E. M. van Cann, "Free vascularized flaps for reconstruction of the mandible: Complications, success, and dental rehabilitation," *J. Oral Maxillofacial Surg.*, vol. 70, pp. 1692–1698, Jul. 2012.

[4] A. K. Antony, W. F. Chen, A. Kolokythas, K. A. Weimer, and M. N. Cohen, "Use of virtual surgery and stereolithography-guided osteotomy for mandibular reconstruction with the free fibula," *Plastic Reconstructive Surg.*, vol. 128, pp. 1080–1084, Nov. 2011.

[5] S. Bai, B. Bo, Y. Bi, B. Wang, J. Zhao, Y. Liu, Z. Feng, H. Shang, and Y. Zhao, "CAD/CAM surface templates as an alternative to the intermediate wafer in orthognathic surgery," *Oral Surg., Oral Med., Oral Pathol., Oral Radiol., Endodontology*, vol. 110, pp. e1–e7, Nov. 2010.

[6] C. G. Lim, D. I. Campbell, and D. M. Clucas, "Rapid prototyping technology in orbital floor reconstruction: Application in three patients," *Craniomaxillofacial Trauma Reconstruction*, vol. 7, pp. 143–146, Jun. 2014.

[7] J. P. Levine, A. Patel, P. B. Saadeh, and D. L. Hirsch, "Computer-aided design and manufacturing in craniomaxillofacial surgery: The new state of the art," *J. Craniofacial Surg.*, vol. 23, pp. 288–293, Jan. 2012.

[8] Z. Dong, B. Li, R. Xie, Q. Wu, L. Zhang, and S. Bai, "Comparative study of three kinds of fibula cutting guides in reshaping fibula for the reconstruction of mandible: An accuracy simulation study in vitro," *J. Cranio-Maxillofacial Surg.*, vol. 45, no. 8, pp. 1227–1235, Aug. 2017.

[9] Z. Dong, Q. Li, S. Bai, and L. Zhang, "Application of 3-dimensional printing technology to Kirschner wire fixation of adolescent condyle fracture," *J. Oral Maxillofacial Surg.*, vol. 73, no. 10, pp. 1970–1976, Oct. 2015.

[10] Z. Dong, Q. Li, L. Zhang, X. Bai, K. Qin, Y. Tian, R. Zhao, S. Liu, J. Wang, and Z. Zhao, "Accuracy of two midsagittal planes in three-dimensional analysis and their measurement in patients with skeletal mandibular deviation: A comparative study," *Brit. J. Oral Maxillofacial Surg.*, vol. 56, no. 7, pp. 600–606, 2018. doi: 10.1016/j.bjoms.2018.06.009.

[11] C. S. Huang and Y. R. Chen, "Orthodontic principles and guidelines for the surgery-first approach to orthognathic surgery," *Int. J. Oral Maxillofacial Surg.*, vol. 44, pp. 1457–1462, Dec. 2015.

[12] J. J. Fang, Y.-H. Tu, T.-Y. Wong, J.-K. Liu, Y.-X. Zhang, and K.-C. Chen, "Evaluation of mandibular contour in patients with significant facial asymmetry," *Int. J. Oral Maxillofacial Surg.*, vol. 45, pp. 922–931, Jul. 2016.

[13] S. Tyan, H. S. Park, M. Janchivdorj, S. H. Han, S. J. Kim, and H. W. Ahn, "Three-dimensional analysis of molar compensation in patients with facial asymmetry and mandibular prognathism," *Angle Orthodontist*, vol. 86, pp. 421–430, Jul. 2015.

[14] Y. Q. Zhang, Y. X. Bai, and N. Zhang, "Evaluation of craniofacial midsagittal plane selection based on cone beam computed tomography," *Beijing J. Stomatology*, vol. 21 pp. 277–280, Jun. 2013.

[15] Y. J. Chen, C.-C. Yao, Z.-C. Chang, H.-H. Lai, S.-C. Lu, and S.-H. Kok, "A new classification of mandibular asymmetry and evaluation of surgical-orthodontic treatment outcomes in Class III malocclusion," *J. Cranio-Maxillofacial Surg.*, vol. 44, pp. 676–683, Jun. 2016.

[16] S. X. Liu, "Symmetry and asymmetry analysis and its implications to computer-aided diagnosis: A review of the literature," *J. Biomed. Inform.*, vol. 42, no. 6, pp. 1056–1064, Dec. 2009.

[17] Q. Hu and W. L. Nowinski, "Radiological symmetry of brain and head images: Comparison and applications," *Int. J. Comput. Assist. Radiol. Surg.*, vol. 1, no. 2, pp. 75–81, Aug. 2006.

[18] S. A. Jayasuriya and A. W.-C. Liew, "Symmetry incorporated fuzzy C-means method for image segmentation," in *Proc. IEEE Int. Conf. Fuzzy Syst.*, Jul. 2013, pp. 1–7.

[19] P. Kalavathi, M. Senthamilselvi, and V. Prasath, "Review of computational methods on brain symmetric and asymmetric analysis from neuroimaging techniques," *Technologies*, vol. 5, no. 2, pp. 16–26, 2017.

[20] M. E. Brummer, "Hough transform detection of the longitudinal fissure in tomographic head images," *IEEE Trans. Med. Imag.*, vol. 10, no. 1, pp. 74–81, Mar. 1991.

[21] F. Baji, M. Mocanu, and D. Popa, "Detection the mid-sagittal plane in brain slice MR images by using local ternary pattern," in *Proc. Int. Conf. Develop. Appl. Syst.*, May 2018, pp. 138–143.

[22] U. Ramasamy, and G. Arulprakash, "Mid-sagittal plane detection in brain magnetic resonance image based on multifractal techniques," *IET Image Process.*, vol. 10, no. 10, pp. 751–762, May 2016.

[23] S. A. Jayasuriya, A. W. C. Liew, and N. F. Law, "Brain symmetry plane detection based on fractal analysis," *Computerized Med. Imag. Graph.*, vol. 37, pp. 568–580, Dec. 2013.

[24] A. Ekin, "Feature-based brain mid-sagittal plane detection by RANSAC," in *Proc. 14th Eur. Signal Process. Conf.*, Sep. 2006, pp. 1–4.

[25] Q. Hu and W. L. Nowinski, "A rapid algorithm for robust and automatic extraction of the midsagittal plane of the human cerebrum from neuroimages based on local symmetry and outlier removal," *NeuroImage*, vol. 20, pp. 2153–2165, Dec. 2003.

[26] I. Volkau, B. Prakash, A. Ananthasubramaniam, V. Gupta, A. Aziz, and W. L. Nowinski, "Quantitative analysis of brain asymmetry by using the divergence measure: Normal-pathological brain discrimination," *Academic Radiol.*. vol. 13, pp. 752–758, Jun. 2006.

[27] L. Liang, K. Rehm, R. P. Woods, and D. A. Rottenberg, "Automatic segmentation of left and right cerebral hemispheres from MRI brain volumes using the graph cuts algorithm," *NeuroImage*, vol. 34, pp. 1160–1170, Feb. 2007.

[28] E. Song, Q. Wang, and G. Ma, "Symmetry analysis to detect pathological brain in MRI," in *Proc. Int. Symp. Multispectral Image Process. Pattern Recognit.*, Nov. 2007, Art. no. 67891F.

[29] F. P. G. Bergo, A. X. Falcão, C. L. Yasuda, and G. C. S. Ruppert, "Fast, accurate and precise mid-sagittal plane location in 3D MR images of the brain," in *Proc. Int. Joint Conf. Biomed. Eng. Syst. Technol.*, Jan. 2008, pp. 278–290.

[30] L. Teverovskiy, and Y. Li, "Truly 3D midsagittal plane extraction for robust neuroimage registration," in *Proc. 3rd IEEE Int. Symp. Biomed. Imag.*, Arlington, VA, USA, Apr. 2006, pp. 860–863.

[31] H. J. Kuijf, S. J. van Veluw, M. I. Geerlings, M. A. Viergever, G. J. Biessels, and K. L. Vincken, "Automatic extraction of the midsagittal surface from brain MR images using the Kullback-Leibler measure," *Neuroinformatics*, vol. 12, pp. 395–403, Jul. 2014.

[32] H. Wu, D. Wang, L. Shi, Z. Wen, and Z. Ming, "Midsagittal plane extraction from brain images based on 3D SIFT," *Phys. Med. Biol.*, vol. 59, p. 1367, Feb. 2014.

[33] H. Wu, D. Wang, L. Shi, Z. Wen, and Z. Ming, "Fast and robust symmetry detection for brain images based on parallel scale-invariant feature transform matching and voting," *Int. J. Imag. Syst. Technol.*, vol. 23, pp. 314–326, Dec. 2013.

[34] Y. Liu and B. M. Dawant, "Automatic localization of the anterior commissure, posterior commissure, and midsagittal plane in MRI scans using regression forests," *IEEE J. Biomed. Health Inform.*, vol. 19, no. 4, pp. 1362–1374, Jul. 2015.

[35] P. Kalavathi and V. B. S. Prasath, "Automatic segmentation of cerebral hemispheres in MR human head scans," *Int. J. Imag. Syst. Technol.*, vol. 26, pp. 15–23, May 2016.

[36] A. G. Schwing and Y. Zheng, "Reliable extraction of the mid-sagittal plane in 3D brain MRI via hierarchical landmark detection," in *Proc. IEEE 11th Int. Symp. Biomed. Imag. (ISBI)*, May 2014, pp. 213–216.

[37] S. A. Jayasuriya and A. W.-C. Liew, "Symmetry plane detection in neuroimages based on intensity profile analysis," in *Proc. Int. Symp. Inf. Technol. Med. Educ.*, Aug. 2012, pp. 599–603.

[38] G. C. S. Ruppert, L. Teverovskiy, C.-P. Yu, A. X. Falcão, and Y. Liu, "A new symmetry-based method for mid-sagittal plane extraction in neuroimages," in *Proc. IEEE Int. Symp. Biomed. Imag.*, Chicago, IL, USA, Apr. 2011, pp. 285–288.

[39] B. A. Ardekani, J. Kershaw, M. Braun, and I. Kanuo, "Automatic detection of the mid-sagittal plane in 3-D brain images," *IEEE Trans. Med. Imag.*, vol. 16, no. 6, pp. 947–952, Dec. 1997.

[40] Y. Liu, R. T. Collins, and W. E. Rothfus, "Automatic extraction of the central symmetry (mid-sagittal) plane from neuroradiology images," Robot. Inst., Carnegie Mellon Univ., Tech. Rep., 1996.

[41] F. Kruggel and D. Y. von Cramon, "Alignment of magnetic-resonance brain datasets with the stereotactical coordinate system," *Med. Image Anal.*, vol. 3, pp. 175–185, Jun. 1999.

[42] Y. Liu, R. T. Collins, and W. E. Rothfus, "Robust midsagittal plane extraction from normal and pathological 3-D neuroradiology images," *IEEE Trans. Med. Imag.*, vol. 20, no. 3, pp. 175–192, Mar. 2001.
[43] Y. Zhang and Q. Hu, "A PCA-based approach to the representation and recognition of MR brain midsagittal plane images," in *Proc. 30th IEEE Annu. Int. Conf. Eng. Med. Biol. Soc.*, Aug. 2008, pp. 3916–3919.
[44] A. V. Tuzikov, O. Colliot, and I. Bloch, "Brain symmetry plane computation in MR images using inertia axes and optimization," in *Proc. 16th Int. Conf. Pattern Recognit.*, Aug. 2002, Art. no. 10516.
[45] A. V. Tuzikov, O. Colliot, and I. Bloch, "Evaluation of the symmetry plane in 3D MR brain images," *Pattern Recognit. Lett.*, vol. 24, pp. 2219–2233, Oct. 2003.
[46] X. Qi, A. Belle, S. Shandilya, W. Chen, C. Cockrell, Y. Tang, K. R. Ward, R. H. Hargraves, and K. Najarian, "Ideal midline detection using automated processing of brain CT image," *Open J. Med. Imag.*, vol. 3, pp. 51–53, Jun. 2013.
[47] S. Prima, S. Ourselin, and N. Ayache, "Computation of the mid-sagittal plane in 3-D brain images," *IEEE Trans. Med. Imag.*, vol. 21, no. 2, pp. 122–138, Feb. 2002.
[48] R. Zhang, T. Sato, and H. Arisawa, "Symmetry recognition using midsagittal plane extraction and tilt correction in 3D head images," in *Proc. SICE Annu. Conf.*, Sep. 2013, pp. 761–766.
[49] M. B. Stegmann, K. Skoglund, and C. Ryberg, "Mid-sagittal plane and mid-sagittal surface optimization in brain MRI using a local symmetry measure," *Med. Image Process., Int. Soc. Opt. Photon.*, vol. 29, pp. 568–580, Apr. 2005.
[50] S. H. Davarpanah and A. W.-C. Liew, "Brain mid-sagittal surface extraction based on fractal analysis," *Neural Comput. Appl.*, vol. 30, no. 1, pp. 153–162, Jul. 2018.
[51] S. An, J.-Y. Lee, C. J. Chung, and K.-H. Kim, "Comparison of different midsagittal plane configurations for evaluating craniofacial asymmetry by expert preference," *Amer. J. Orthodontics Dentofacial Orthopedics*, vol. 152, no. 6, pp. 788–797, Dec. 2017.
[52] R. Adams and L. Bischof, "Seeded region growing," *IEEE Trans. Pattern Anal. Mach. Intell.*, vol. 16, no. 6, pp. 641–647, Jun. 1994.
[53] W. J. Tan, Y. Yuan, A. Chen, L. Mao, Y. Ke, and X. Lv, "An approach for pulmonary vascular extraction from chest CT images," *J. Healthcare Eng.*, vol. 2019, Jan. 2019, Art. no. 9712970. doi: 10.1155/2019/9712970.
[54] W. Tan, J. Yang, Z. Bian, Z. Gong, and D. Zhao, "Automatic extraction of 3d airway tree from multislice computed tomography images," *J. Med. Imag. Health Inform.*, vol. 4, no. 5, pp. 768–775, Oct. 2014.
[55] S. Gottschalk, M. C. Lin, and D. Manocha, "OBBTree: A hierarchical structure for rapid interference detection," in *Proc. 23rd Annu. Conf. Comput. Graph. Interact. Techn.*, Aug. 1996, pp. 171–180.
[56] S. Yu and T.-Z. Huang, "Exponential weighted entropy and exponential weighted mutual information," *Neurocomputing*, vol. 249, pp. 86–94, Aug. 2017.
[57] F. Escolano, E. R. Hancock, M. A. Lozano, and M. Curado, "The mutual information between graphs," *Pattern Recognit. Lett.*, vol. 87, pp. 12–19, Feb. 2017.
[58] T. M. Cover and J. A. Thomas, *Elements of Information Theory*. Hoboken, NJ, USA: Wiley 2012.
[59] G. Gao, C. Wen, and H. Wang, "Fast and robust image segmentation with active contours and Student's-t mixture model," *Pattern Recognit.*, vol. 63, pp. 71–86, Mar. 2017.

WENJUN TAN received the M.S. and Ph.D. degrees in pattern recognition and intelligent system from the Northeastern University, Shenyang, China, in 2007 and 2010, respectively. He is currently an Associate Professor with the School of Computer Science and Engineering, Northeastern University. He has authored or coauthored more than 50 international research papers, and holds 16 patents. His current research interests include medical image processing and computer-aided diagnosis.

YING KANG received the B.S. degree in school of computer science and engineering from the Northeastern University, China, in 2013. He is currently pursuing the master's. degree with the Sino-Dutch Biomedical and Information Engineering School, Northeastern University, China. His research interests include medical image processing and computer algorithm.

ZHIWEI DONG received the M.D. and Ph.D. degrees in oral and maxillofacial surgery from the Fourth Military Medical University, Xi'an, in 2008 and 2011, respectively. Since 2011, he has been an Attending Doctor with the General Hospital of Shenyang Military Command. He has authored more than 10 articles and more than two patents. His research interests include oral and maxillofacial surgery, and digital oral surgery.

CHAO CHEN received the bachelor's degree in automation and master's degree in pattern recognition and intelligent system from the Northeastern University, Shenyang, China, in 2005 and 2008, respectively, and the Ph.D. degree from Tokyo Institute of Technology, Japan. Currently, he is an Associate Professor with the School of Electrical and Electronic Engineering, Tianjin University of Technology. His research interests include pattern recognition and intelligent algorithm, invasive and non-invasive brain-computer interface (BCI), medical image processing, and robot control.

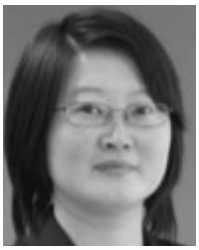

XIAOXIA YIN received the Ph.D. degree in electronics engineering from The University of Adelaide, Australia. She was a Visiting Scholar with the University of Reading, Reading, U.K., under the supervision of S. Hadjiloucas, and with the University of Cambridge, Cambridge, U.K., under the supervision of L. F. Gladden. She involved in tumor detection via DCE-MRI with The University of Melbourne, Australia, under the supervision of Prof. Kotagiri. She has an existing collaboration with Prof. M.-Y. Su with the Center for Functional Onco Imaging, University of California at Irvine, USA, and with Prof. T. Kron with the Peter MacCallum Cancer Centre, Australia. She is currently a Research Fellow in high-dimensional medical image analysis with Victoria University, Australia. Her research interests include multiresolution analysis, segmentation, image reconstruction and classification, and their applications to high-dimensional medical imaging. She was a member of the Organizing Committee and the Publication Chairperson of the 3rd International Conference of Health Information Science, and a member of the Organizing Committee and the Program Co-Chairperson of the 4th and 5th International Conference of Health Information Science. She received the Postdoctoral Research Fellowship from the Australian Research Council, in 2009. She is the Managing Editor of the *Health Information Science and System Journal*.

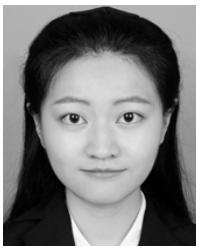

YING SU received the B.S. degree in automation from the Northeastern University, Liaoning Province, China, in 2017. She is currently pursuing the M.S. degree with Sino-Dutch Biomedical and Information Engineering, Northeastern University. Her research interests include medical image segmentation and algorithm optimization.

YANCHUN ZHANG is currently the Director of the Centre for Applied Informatics, and coordinates a multidisciplinary e-research program across the Victoria University. He is also an International Research Leader in databases, data mining, health informatics, Web information systems, and Web services. He has authored over 220 research papers in international journals and conferences proceedings, and authored/edited 12 books. His major research interests include data mining, pattern recognition, machine learning, biomedical signal processing, databases, data management, e-health, environmental studies, and sensor networks. He is the Editor-in-Chief of *World Wide Web Journal* (Springer) and the Health Information Science and Systems. He is also the Chairman of the International Web Information Systems Engineering Society.

LI ZHANG received the M.D. degree in oral and maxillofacial surgery from the Fourth Military Medical University, Xi'an, in 1999, and the Ph.D. degree in oral and maxillofacial surgery from China Medical University, Shenyang, in 2006. From 1992 to 1998, he was a Resident Doctor and from 1998 to 2012, he was an Attending Doctor with the General Hospital of Shenyang Military Command. Since 2012, he has been an Associate Chief of Doctor with the General Hospital of Shenyang Military Command. He has authored two books, more than 20 articles, and more than three patents. His research interests include oral and maxillofacial surgery and digital oral surgery.

LISHENG XU received the B.S. degree in electrical power system automation, the M.S. degree in mechanical electronics, and the Ph.D. degree in computer science and technology from Harbin Institute of Technology, Harbin, China, in 1998, 2000, and 2006, respectively. He is currently a Full Professor with the Sino-Dutch Biomedical and Information Engineering School, Northeastern University, China. He has authored or coauthored more than 100 international research papers, and holds 15 patents and four pending patents. His current research interests include nonlinear medical signal processing, computational electromagnetic simulation, medical imaging, and pattern recognition. He is the Director of Theory and Education Professional Committee of China Medical Informatics Association. He is the Senior Member of Chinese Society of Biomedical Engineering. He is the member of the editorial board for many international journals such as *Physiological Measurement, Biomedical Engineering Online, Computers in Biology and Medicine*, and so on.